Combined Atomic Force Microscopy and Modeling Study of The Evolution of Octadecylamine Films on a Mica Surface

K. G. Patil,[†] V. Santhanam,[†] S. K. Biswas,[‡] and K. G. Ayappa*,[†]

Department of Chemical Engineering, and Department of Mechanical Engineering, Indian Institute of Science, Bangalore 560012, India

Received: September 7, 2009; Revised Manuscript Received: January 4, 2010

The time evolution of the film thickness and domain formation of octadecylamine molecules adsorbed on a mica surface is investigated using atomic force microscopy. The adsorbed film thickness is determined by measuring the height profile across the mica−amine interface of a mica surface partially immersed in a 15 mM solution of octadecylamine in chloroform. Using this novel procedure, adsorption of amine on mica is found to occur in three distinct stages, with morphologically distinct domain formation and growth occurring during each stage. In the first stage, where adsorption is primarily in the thin-film regime, an average film thickness of 0.2 (±0.3) nm is formed for exposure times below 30 s and 0.8 (±0.2) nm for 60 s of immersion time. During this stage, large sample spanning domains are observed. The second stage, which occurs between 60−300 s, is associated with a regime of rapid film growth, and the film thickness increases from about 0.8 to 25 nm during this stage. Once the thick-film regime is established, further exposure to the amine solution results in an increase in the domain area, and a regime of lateral domain growth is observed. In this stage, the domain area coverage grows from 38 to 75%, and the FTIR spectra reveal an increased level of crystallinity in the film. Using a diffusion-controlled model and a two-step Langmuir isotherm, the time evolution of the film growth is quantitatively captured. The model predicts the time at which the thin to thick film transition occurs as well as the time required for complete film growth at longer times. The Ward−Tordai equation is also solved to determine the model parameters in the monolayer (thin-film) regime, which occurs during the initial stages of film growth.

Introduction

Surface modification by adsorption of molecules from solution has a wide range of technological applications such as mineral flotation,[1,2] nanotribology,[3,4] detergency, and corrosion inhibition.[5,6] Surface functionalization allows control of surface wettability and chemical specificity to other molecules, leading to diagnostic and patterning possibilities for biosensors[7] and microelectronics. The hydrophilic head groups of the molecule chemisorb on a charged solid surface to provide load bearing in boundary lubrication, while the hydrophobic tails often become antifriction agents.[6] There is another family of functionalizers where the head groups may bind weakly to the metal surface while the backbone and the tail group provide functions such as corrosion inhibition,[8,9] antifoaming, and detergency.[10–12] Amine-based molecules are one such group which are particularly effective in detergency as their physisorbed states allow the deposit and the surfactant to be easily washed away in a rinsing step. Although there exists a wide body of literature on the adsorption kinetics and film growth of chemisorbed self-assembling films,[13,14] physisorbed films have received less attention. In this paper, we study the growth kinetics of an amine-based molecule physisorbed on a mica surface with particular emphasis on determining the film thickness and its associated morphology as a function of time.

Surface-active molecules diffuse from the solution to the solid substrate, where they adsorb to form crystalline domains. The domains or islands grow laterally until complete monolayer coverage is achieved after a sufficiently long exposure time.[15] The kinetics are found to be dependent on the chemical and physical nature of the substrate, the presence of water, the temperature, the pH of the solvent, and the structure of surfactant molecules. The growth mechanism changes when the molecules are physisorbed, and multilayer structures become possible. In the absence of a chemical bond, electrostatic and van der Waals interactions define the interaction strength during the adsorption of surfactants, proteins,[16,17] and polymers onto the surfaces.[18] Measurement of surface forces generated by adsorbed ethoxylated amine surfactants on mica[8] showed that the physical status of the deposit depends on both the concentration and solution pH. When the pH is low (<8), the interaction is electrostatic, and densely packed amine monolayers render the mica surface hydrophobic. At higher pH values between 9 and 11, the surface is rendered hydrophilic.[8] The increased hydrophilicity is attributed to the formation of bilayers and disordered monolayers.

AFM has been used to study the structure of quaternary ammonium surfactants on mica from aqueous solutions.[18–22] Above the critical micellar concentration, noncontact AFM measurements reveal the presence of cylindrical micelles on the mica surface and hemimicelles on hydrophobic surfaces such as graphite.[19,21] Cylindrical structures were not observed below the critical micellar concentration in the contact mode AFM.[22] In other studies, the Kraft temperature was found to play an important role. Above the Kraft point of C_{14}TAB, micellar structures were observed on the mica surface, and below the Kraft point, adsorption occurred by 2D island formation and growth. Increasing the alkyl chain length (>14) was found to

* To whom correspondence should be addressed. E-mail: ayappa@chemeng.iisc.ernet.in.
[†] Department of Chemical Engineering.
[‡] Department of Mechanical Engineering.

10.1021/jp9086255
Published on Web 02/04/2010

favor monolayer formation.[18] The morphology of amine molecules deposited from chloroform[23,24] and ethanol has also been studied using AFM.[25] Deposition time and humidity were found to influence growth morphology of the physisorbed monolayers of amine deposited from chloroform, while multilayer architecture was observed when mica was immersed in ethanol containing octadecylamine molecules. The polarity of the solution is thus an important factor which contributes to the film architecture.[25] The formation of multilayers was inferred from the presence of steps detected in the AFM topographical data, and the presence of a micellar phase was associated with the formation of multilayers.[25] Key problems encountered in studying the multilayer architecture of deposited films are associated with the determination of the adsorbed film thickness. The AFM experiments yield relative height differences between the domains. In the work by Benitez et al.,[25] step heights larger than the molecular length were attributed to multilayer formation. The thickness of surface adsorbed films is usually determined using ellipsometry.[26] However when mica is used as a substrate, measurements using ellipsometry are marked by the diffraction interference from optically transparent mica layers. Hence, only a few studies have recently reported the surface excess adsorbed on mica using ellipsometry.[16,27]

The rate of adsorption of the molecules on the solid substrate competes with the rate of diffusion of the molecules through the solvent media in yielding a specific three-dimensional architecture of the surfactant molecules. The adsorption of molecules from solution onto a solid surface can be studied using the diffusion equation which yields the time evolution of surface coverage as well as the concentration variation in the liquid film adjacent to the surface.[28,29] For a surface exposed to an infinite liquid bath containing the surface-active species, the diffusion equation reduces to the Ward−Tordai equation, which is an integral equation for the surface coverage.[30] If diffusion is the rate-limiting step, then the adsorbed surface concentration is assumed to be in equilibrium with the concentration of the species adjacent to the surface. If the kinetics of adsorption and desorption are slow compared to the diffusion of molecules to the surface, then a suitable kinetic model must be incorporated at the solid−liquid interface.[31] The primary thermodynamic input into these models is the adsorption isotherm for the system under consideration. Adsorption of $C_{10}E_8$ surfactant at the liquid−air interface has been investigated for a pendant drop geometry using tensiometry experiments as well as a finite element solution of the diffusion equation to take into account the drop geometry.[32] The study indicates that the process is diffusion-controlled at low surfactant concentrations and shifts to a mixed diffusive-kinetic-controlled regime at higher concentrations. Using a Langmuir adsorption isotherm, diffusion-controlled adsorption of binary surfactant mixtures of laurate/sodium myristate below the critical micellar concentration have been studied.[33] Such models use the Langmuir isotherm and explore the adsorption dynamics in the monolayer regime.

In this work, we use the AFM to record ex situ growth of an amine film from a chloroform solution. The growth process is studied as a function of immersion time. A novel AFM procedure is used to determine the film thickness by recording the height of the adsorbed film on a mica surface that is partially immersed in solution. The procedure provides a direct measurement of the thickness of the adsorbed film by using the bare mica surface as a reference. Using this procedure, we are able to measure film thickness ranging from 0.2 to 26 nm. The height variations with immersion time are correlated with the structural evolution and distribution of domains as a function of time. The time evolution of the experimentally observed film thickness variation is modeled by solving both the Ward−Tordai and the diffusion equation.

Experimental Section

Materials and Sample Preparation. Freshly cleaved muscovite mica was used as a substrate for the octadecylamine ($NH_2-(CH_2)_{17}-CH_3$) deposition. Octadecylamine (Fluka >99.9%) was used as received, and chloroform (Aldrich, 99.9%, U.S.A.) was used as the solvent. A 15 mM solution of octadecylamine was prepared using chloroform as the solvent. Muscovite mica (4 cm × 1 cm) was repeatedly cleaved on both sides under ambient conditions (20 ± 1) °C, 35−40% relative humidity) with adhesive tape and immediately immersed in 5 mL glass vials containing octadecylamine solution for immersion times which were varied from 30 to 900 s. After exposure to the amine solution, the samples (without rinsing) were directly kept in an airtight vacuum desiccator for 12 h. No trace of solvent droplets could be observed visually on these samples after removing from the solution, indicating that the adsorption occurs only during immersion. In order to provide a reference for determining the thickness of the adsorbed film, two types of immersion protocols were followed. In the first protocol, mica was fully immersed in the amine solution, whereas in the second protocol, mica was only partially immersed in solution with part of the mica sample exposed to air above the air−solution interface. AFM scans were carried out across the marked position of the interface, enabling us to use the bare mica surface as a reference for inferring the thickness of the adsorbed layer. All the glassware used in the experiments were first boiled in HCl followed by a thorough rinse with Millipore water, and subsequently dried overnight in the oven at 100 °C.

Atomic Force Microscopy. Atomic force microscopy experiments were carried out (SPM Explorer, ThermoMicroscope, Santa Barbara, U.S.A.) in contact mode with Si_3N_4 pyramidal tips (Veeco) with a nominal 30−40 nm tip diameter and a 0.15 N m^{-1} normal spring constant. The tip diameter and AFM were calibrated using standard gratings (NT-MDT TGT1, Russia). A single AFM was used to gather the topographical and frictional information and force−distance curves. Before each experiment, the tip was kept in ethanol for 180 s and then exposed to UV radiation (Bioforce Nanoscience, U.S.A.) for 20 min. All experiments were carried out at room temperature (20 ± 1 °C) and at 35% relative humidity. All AFM scans were carried out at ∼5.0 nN normal load with the AFM kept on a floating air table. All of the atomic force microscopy (AFM) images were processed with first-order correction to remove basal tilt in the image using the WSxM software.[34] The % domain area was also calculated using the WSxM software. Using this software, the domain area was flooded, and the % of area covered by domains was calculated. While gathering topographical and friction images, the smaller scan areas of 2 × 2 μm as well as larger-area scans of ≥5 × 5 μm were used. The film thickness was calculated by processing the height histogram from the AFM image. The height histogram consists of two peaks, one corresponding to the bare mica and the second corresponding to the amine film. Each histogram was fitted to a Gaussian, and the difference in the mean heights was reported as the film thickness. While evaluating the film thickness across the amine−mica interface, larger scan areas of ≥10 × 10 μm were used. The height histograms were recorded only after the line scans yielded a reliable and clear height difference across the interface.

TABLE 1: Integral Intensities for Octadecylamine on a Mica Surface at Different Immersion Times for the Antisymmetric Methylene (d^-) Peak

immersion time (s)	integral intensity
30	0.0451
300	0.1954
900	0.5908

Fourier Transform Infrared Spectroscopy. All spectra were acquired by infrared reflection absorption spectroscopy (IRAS) in a Perkin−Elmer GX spectrometer equipped with a liquid-nitrogen-cooled mercury cadmium telluride (MCT) detector. All IR spectra reported were referenced to a bare mica substrate and acquired over 2012 scans at 4 cm^{-1} resolution with a p-polarized IR beam. The sample chamber and detector were purged for 20 min with dry nitrogen before the start of the experiment. Purging was also carried out for a duration of 5 min at regular intervals of 30 min during the experiment. Spectra were collected with a heating accessory (Harrick, New York, U.S.A.) with an incident angle of 75° normal to the surface. Built-in software was used to calculate the full width at half-maxima (fwhm) values as well as the integral intensity (Table 1). To prevent the interference fringes that occur due to reflections from the layered structure of mica, it was critical to cleave the mica sample down to a few micrometers thick.[35]

Contact Angle. To qualitatively assess the hydrophilic and hydrophobic nature of the surface, we have performed sessile contact angle measurements of water drops on samples prepared using the partially immersed protocol. These experiments were carried out on the OCA-35 goniometer. Water drops were generated with a needle of 0.52 mm outer diameter. The amount of water used in each drop was constant (7 μL) at a discharge rate of 0.5 μL per second.

Results

Fourier Transform Infrared Spectroscopy (FTIR). FTIR spectra of the amine films on mica are shown in Figure 1 for different immersion times. In all cases, both the CH_2 antisymmetric (d^-) and CH_2 symmetric (d^+) peak positions are clearly observed. As the immersion time is increased, the antisymmetric stretch shifts from 2920 to 2916 cm^{-1}, indicating a greater degree of ordering in the film at longer immersion times. The peak positions at 900 s for both the antisymmetric (2916) and symmetric (2849) modes are similar to those observed for alkanethiol molecules adsorbed on gold.[36,37] Increasing the immersion time also increases the intensity of both the symmetric and antisymmetric peaks. An increase of almost 2 orders of magnitude is observed in the integral intensities from 30 to 900 s immersion times. This provides the first qualitative signature of an increase in the amount of amine molecules adsorbed on the surface.

Film Thickness Measurements. To investigate the film thickness evolution as a function of immersion time, we carried out AFM experiments where the mica surface was only partially immersed in the amine solution. Evolution of the film thickness was investigated by recording the topographical changes across the mica−amine film interface in a specimen. A typical AFM image is shown in Figure 2 for an immersion time of 180 s. A distinct boundary between the adsorbed film and the bare mica surface can be observed in the image. In this case, the height histograms corresponding to the bare mica and amine film are well-defined, and the interface height is obtained from the difference between the mean values of the histograms. A similar procedure was adopted for obtaining the interface height at

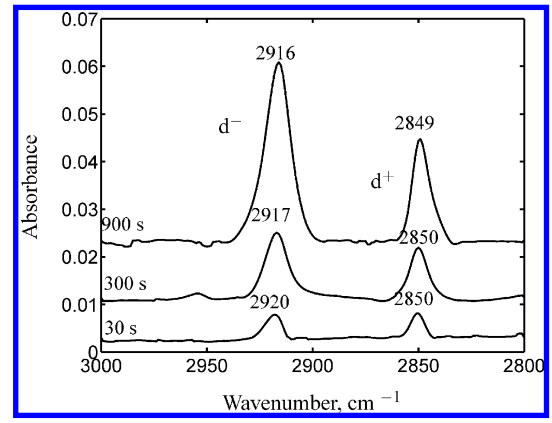

Figure 1. FTIR spectra indicating the symmetric (d^+) and antisymmetric (d^-) methylene peaks of octadecyl amine on mica for different immersion times. Amine molecules are more ordered as the immersion time is increased. The integral intensities are given in Table 1.

immersion times greater than 120s (Figure S1Supporting Information), where well-defined mica−amine interfaces were observed. We note that at the short immersion times where the interface heights were less than 1 nm, well-separated height histograms could not be resolved. In these situations, the interface heights were obtained from averaging the height differences from a large number of line scans across the interface. An example of this situation at 30 s of immersion time is illustrated in Figure S1 of the Supporting Information. Figure 3 summarizes the amine film thickness variation for immersion times in a 30−900 s range. Upon examining the data plotted in Figure 3, three distinct regimes of film growth are identified. At short times, denoted as stage I (Figure 3), the thickness of the adsorbed film is below 1 nm. We refer to this as the thin-film regime. Above 60 s, denoted as stage II, a rapid increase in film growth takes place, reaching a maximum height of 26 ± 3 nm. The transition from a thin to thick film occurs between 60 and 180 s, and the film growth is complete at about 300 s. Above 300 s, the film thickness is more or less unchanged.

In order to check if the equilibrium film thickness observed in stage III was limited by the amount of amine molecules available in solution, we carried out experiments with a larger solution vial containing twice the solution volume (10 mL). The film thickness measured after 900 s of immersion time in the larger vials was 25.0 ± 4 nm. This indicates that the amount of solution used contains a sufficient amount of amine molecules for complete film formation.

Domain Area Coverage. Figure 4 shows the LFM images for immersion times ranging from 30 to 900 s for small (2 × 2 μm) scan areas. The morphology of the film after 30 s of immersion (Figure 4a) shows large "sample spanning" domains which cover about 70% of the scanned area. The domains consist of rough edges and hole-like defects. Such rough edges at small immersion times have also been observed for silanes,[26,38] and hole-like defects have been observed in amine films at short immersion times.[39] At immersion times greater than 180 s, the LFM images show a distinctly different morphology of the adsorbed (Figure 4c) amine molecules, different from what was observed at smaller immersion times (Figure 4a and b). The long immersion time images show (Figure 4e and f) well-defined domains. This structure was first observed at an immersion time of 300 s (Figure 4c). As the immersion time was increased beyond 300 s, the size of individual domain grew monotonically, and beyond 600 s, well-defined domains were observed, as seen in Figure 4e and f. The large scan area (>5 × 5 μm^2) images

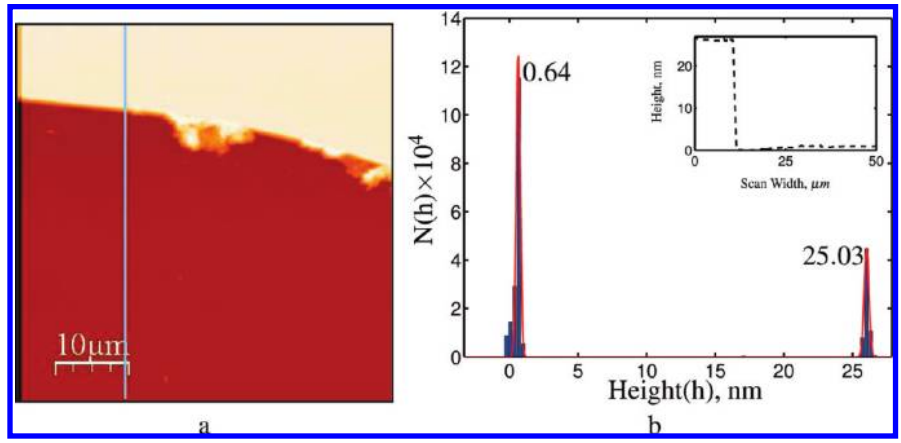

Figure 2. (a) Atomic force microscopy images and (b) histograms for 180 s and obtained using the partially immersed protcol. At these longer immersion times, a well-defined interface is formed, and the difference in the height histograms between the amine and mica surfaces yields a film thickness of 24.4 nm. The insets in (b) show typical height variations corresponding to the lines marked in the AFM image.

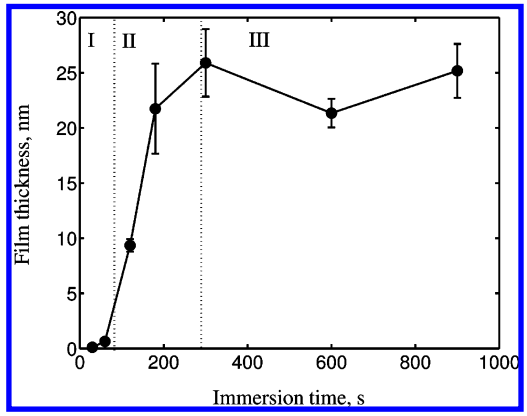

Figure 3. Film thickness variation obtained using the partially immersed samples as a function of immersion time. The data reveal three distinct regimes during the film thickness evolution. Stage I corresponds to short times, where the film corresponds to the thin-film regime. During stage II, a transition from thin to thick film occurs, and stage III corresponds to an adsorbed film of thickness greater than 20 nm.

(Figure S2 of Supporting Information) show morphological variations similar to that observed with the small scan area images ($2 \times 2\ \mu m^2$). Figure 5 shows the average percentage of area covered by the domains as a function of immersion time. The percentage of the surface area covered by domains is minimum at about 300 s of immersion time, a time at which the film thickness also reaches a maximum and a plateau (Figure 3). In both the small and large-area scans, the domain heights recorded were in the range of 1.2−1.5 nm. For the small-area scans, the data represent averages over more than six AFM images from three different experiments. For larger-area scans, the average domain area reported is based on at least four AFM images from two different experiments.

In order to determine whether the regions between the domains formed, for example, at 180 s of immersion were bare mica or not, we obtained force curves at positions A and B, as illustrated in Figure 4b. The pull-off forces recorded at A and B were 12 ± 4 and 17 ± 2 nN, respectively. Similar adhesion forces have been reported for other methyl-terminated SAMs.[40] These adhesion forces are significantly smaller than those of bare mica, 45 ± 9 nN.[41−44] The adhesion data indicate that the dark regions B (or valleys) in Figure 4 are not bare mica surfaces but contain the same molecules as those in the domains (region A). Hence, we conclude that regions A and B both consist of adsorbed amine molecules.

Contact Angle. Images of the water drops placed on bare mica (Figure 6a) and amine films formed with 30 and 180 s of immersion time are shown in Figure 6b and c, respectively. Contact angles on the mica surface show the hydrophilic nature of mica exhibiting contact angles of 20−40°. The drops on the amine side clearly show the hydrophobic nature of the modified substrate giving rise to contact angles of 95−100°. The contact angles are similar both for 30 and 180 s, indicating that the surface energies are similar, despite the large differences in the film thickness at these conditions. Similar contact angles were observed on the amine film at other immersion times. An interesting observation was the movement of a drop toward the hydrophilic surface when placed at the mica−amine interface (not shown). This tendency of the drop to move toward a low contact angle position has been exploited to induce drop movement in surfaces with graded hydrophilicity[45] and provides a macroscopic validation of the formation of the mica−amine interface in our partially immersed experiments. The contact angle measurements establish that the chemistry of the adsorbed film, despite the morphological and topographical heterogeneity observed in the LFM images, are similar.

Model Formulation. In this section, we develop a model to explain the temporal evolution from the thin to thick film transition observed in the AFM experiments. In order to predict the temporal evolution of the adsorbed amine film growth, we solve the 1D diffusion equation across a thin liquid film of thickness L adjacent to the planar mica surface with appropriate boundary and initial conditions. The 1D diffusion equation is

$$\frac{\partial c}{\partial t} = D\frac{\partial^2 c}{\partial z^2} \tag{1}$$

where $c(z, t)$ is the concentration of amine solution in the bulk liquid film and D is the diffusion coefficient of octadecylamine in chloroform. The concentration at the boundary of the liquid film ($z = L$) is assumed to be constant

$$c(z = L, t) = c_0 \tag{2}$$

and at the mica−liquid interface ($z = 0$), the boundary condition is

$$D\left(\frac{\partial c}{\partial z}\right)_{z=0} = \frac{\partial \Gamma}{\partial t} \quad (3)$$

Equation 3 implies that the flux of incoming molecules is equal to the rate of adsorption onto the mica surface. If the surface concentration, Γ, is related to $c(z = 0, t)$ through an adsorption isotherm, then the model implicitly assumes that adsorption is fast compared to diffusion and local equilibrium is rapidly established at the mica surface. An alternative approach is to consider a detailed reaction kinetic mechanism for monolayer and multilayer film growth.[46] The initial conditions are

$$c(z, t = 0) = 0 \quad (4)$$

and

$$\Gamma(t = 0) = 0 \quad (5)$$

If the liquid film is assumed to be semi-infinite and the initial conditions are $c(z, t = 0) = c_0$, then the diffusion equation can be reduced to an integral equation known as the Ward−Tordai equation (eq 6). In this case, the initial concentration of the amine adjacent to the mica surface is the bulk amine concentra-

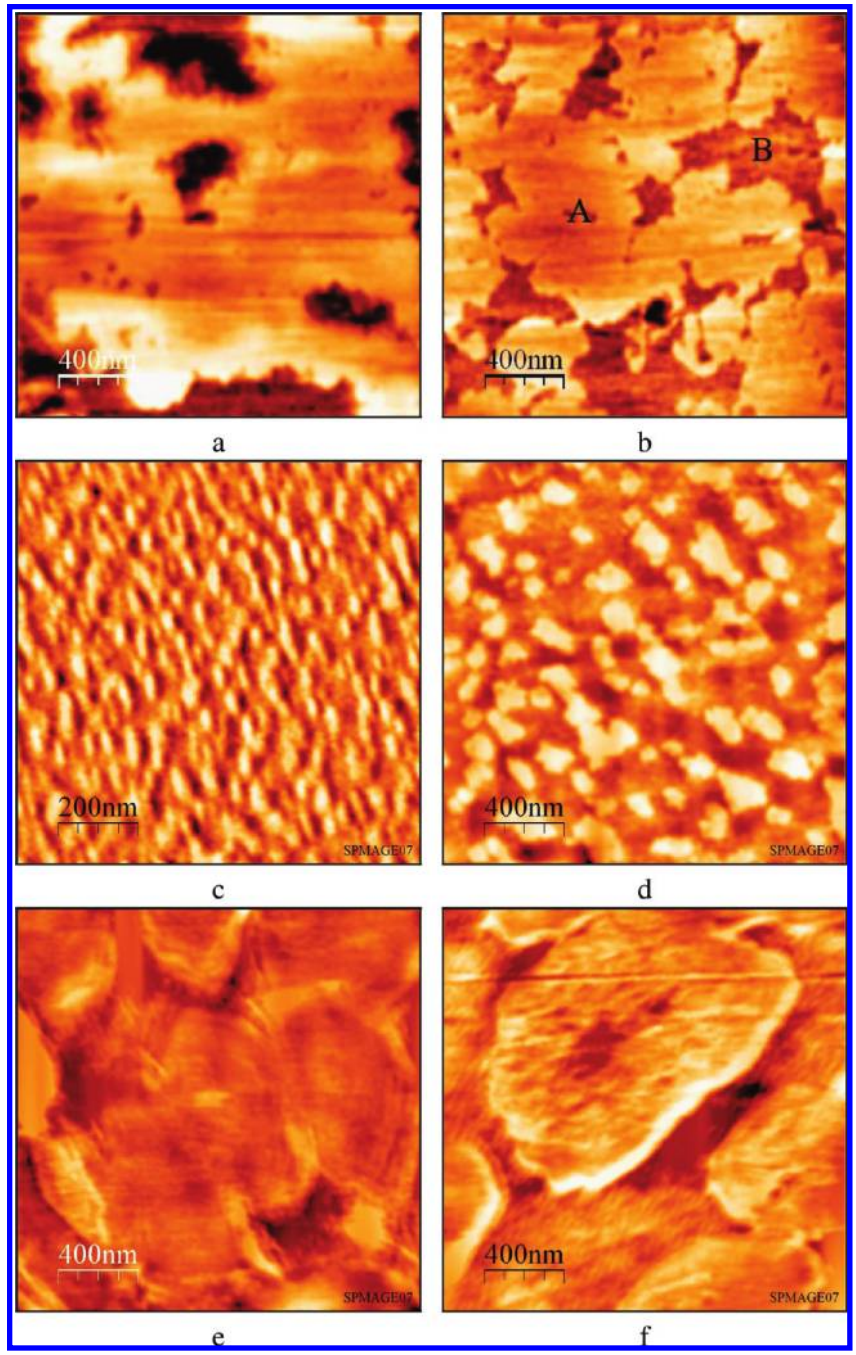

Figure 4. Lateral force microscopy (LFM) images of octadecylamine on mica for different immersion times with small (4 μm^2) scan areas and fully immersed protocol; (a) 30, (b) 180, (c) 300, (d) 420, (e) 600, and (f) 900 s. All scan areas are 2 × 2 μm, except for 300 s, which is 1 × 1 μm. At short times (a and b), large sample spanning domains are observed followed by smaller domain sizes at intermediate times (c and d), which grow in size, giving rise to rounded domains at longer times (e and f).

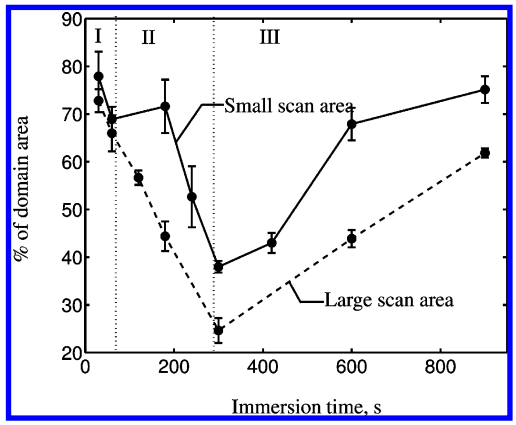

Figure 5. Effect of immersion time on % domain areas for small (2 × 2 μm) as well as large (≥5 × 5 μm) scan areas. At short times (stage I), the domain area reflects the formation of large sample spanning domains. At intermediate times (stage II), a decrease in the domain area is observed, and above 300 s (stage III), the domain size grows monotonically.

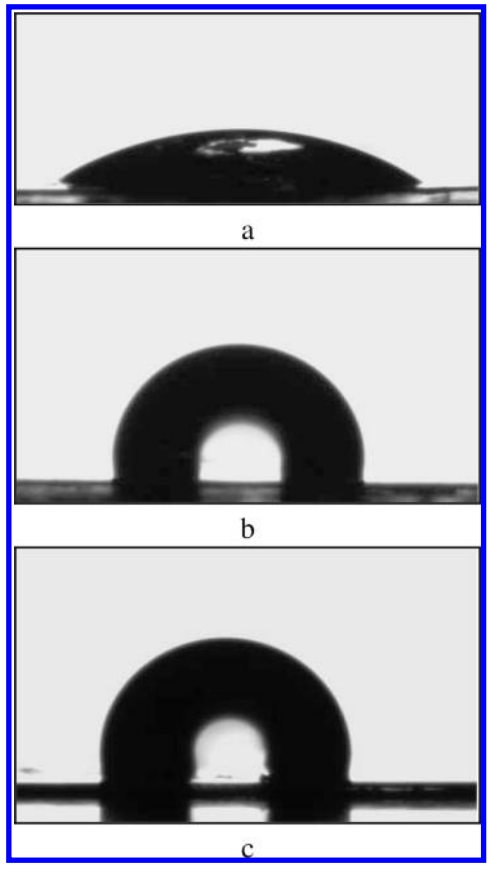

Figure 6. Water drop shapes obtained from goniometer experiments for partially immersed samples for immersion times of 30 s (a) on a mica surface, (b) on an amine domain, and (c) on an amine domain for a 180 s immersion time. The contact angles are 33, 101, and 95° for (a), (b), and (c), respectively.

tion. The Ward−Tordai equation[30] relates the time-dependent adsorbed surface concentration, $\Gamma(t)$, to the bulk concentration of the solute, c, adjacent to the surface

$$\Gamma(t) = \Gamma_0 + 2\sqrt{D}\left[c_0\sqrt{\frac{t}{\pi}} - \int_0^t \frac{c(\tau)}{2\sqrt{\pi(t-\tau)}}\mathrm{d}\tau\right] \quad (6)$$

where Γ_0 is the initial surface concentration, D the diffusion coefficient, and c_0 the corresponding initial concentration. The surface amine concentration, $\Gamma(t)$, is related to the bulk concentration through an appropriate adsorption isotherm. In this manuscript, we consider the Langmuir isotherm to model the surface concentration in the thin-film regime referred to earlier as stage I (Figure 3). The Langmuir isotherm

$$\Gamma = \frac{\Gamma_{m1}c}{c_{l1} + c} \quad (7)$$

where Γ_{m1} and c_{l1} are the two model parameters. Within the Ward−Tordai framework, eqs 6 and 7 must be solved numerically to obtain $\Gamma(t)$, the surface concentration as a function of time. We use a collocation method with a linear basis set that is used in finite element analysis,[47] and the details are available in the Supporting Information. We checked our solution procedure for the Ward−Tordai equation by comparing the solution obtained using the collocation method with the solution reported for the $C_{10}E_8$ surfactant adsorbed at the liquid−air interface, and excellent agreement was obtained.[32]

In order to solve either the Ward−Tordai equation (eq 6) or the diffusion equation (eq 1) the input into the model is an appropriate adsorption isotherm for the surface. In this study, we use a two-site Langmuir model to capture the thin to thick film transition observed in the experimental data. The two-site Langmuir model is

$$\Gamma(t) = \begin{cases} \dfrac{\Gamma_{m1}c}{c_{l1} + c} & \text{if } c \le c_i \\ \dfrac{\Gamma_{m1}c}{c_{l1} + c} + \dfrac{\Gamma_{m2}c}{c_{l2} + c} & \text{if } c \ge c_i \end{cases} \quad (8)$$

where for $c \le c_i$, the adsorption is in the monolayer regime and for $c \ge c_i$, multilayer formation is captured by the isotherm. The two-site model captures the step-like features that have been observed for adsorption of surfactants from solutions onto solid surfaces.[46,48] The additional parameters in the multilayer model are Γ_{m2}, c_{l2}, and c_i (eq 8). The diffusion equation, eq 1, was solved using a finite difference scheme with an implicit time integration. Typical time and space intervals used for these calculations were 0.001 and 0.003 in appropriate reduced units (Supporting Information).

Ward−Tordai Solutions. The primary motivation for using the Ward−Tordai model in the thin-film regime was to establish the parameters Γ_{m1} and c_{l1} in eq 7 and the diffusion coefficient D. The diffusion equation was then used to predict the film thickness variation as a function of time for both the thin- and thick-film regimes. We note that the Ward−Tordai equation can also be solved using the multilayer adsorption model (eq 8); however, this results in a large number of unknown parameters that have to be estimated.

The parameters in the model were estimated in the following manner. On the basis of the formation of a close-packed monolayer structure on the mica surface and using a van der Waals diameter of 0.33 nm[49,50] for the NH_2 head group, $\Gamma_{m1} = 1.74 \times 10^{-3}$ mol m^{-2}. Using this value of Γ_{m1}, we solved the Ward−Tordai equation using the Langmuir isotherm (eq 7) for different values of the parameter c_{l1} and the diffusivity, D. We note that the diffusivity of C_2−C_{18} thiols in ethanol[51] lie in the range of 5.7−9.5 × 10^{-10} m^2 s^{-1}. Figure 7a illustrates the variation of $\Gamma^*(t) = \Gamma/\Gamma_{m1}$ at different values of c_{l1} for $D = 10 \times 10^{-10}$ m^2 s^{-1}. A lower value of c_{l1} increases the amount adsorbed on the surface at long times. From solutions of the

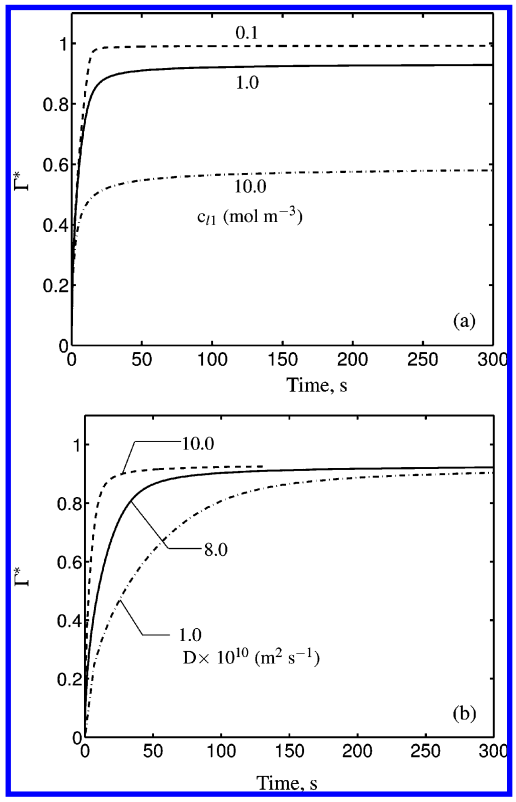

Figure 7. Solutions to the Ward−Tordai equation (eq 6) using the Langmuir isotherm, indicating the effect of (a) the interaction parameter c_{l1} and (b) the diffusion coefficient D on the evolution of the amount adsorbed, $\Gamma^* = \Gamma/\Gamma_{m1}$. For $c_{l1} = 1.0$ mol m^{-3} and $D = 8.0 \times 10^{-10}$ m^2 s^{-1}, maximum coverage is achieved within 60 s of exposure to the amine solution. Parameters used: (a) $D = 10 \times 10^{-10}$ m^2 s^{-1}, $\Gamma_{m1} = 1.74 \times 10^{-3}$ mol m^{-2}; (b) $c_{l1} = 1.0$ mol m^{-3}, $\Gamma_{m1} = 1.74 \times 10^{-3}$ mol m^{-2}.

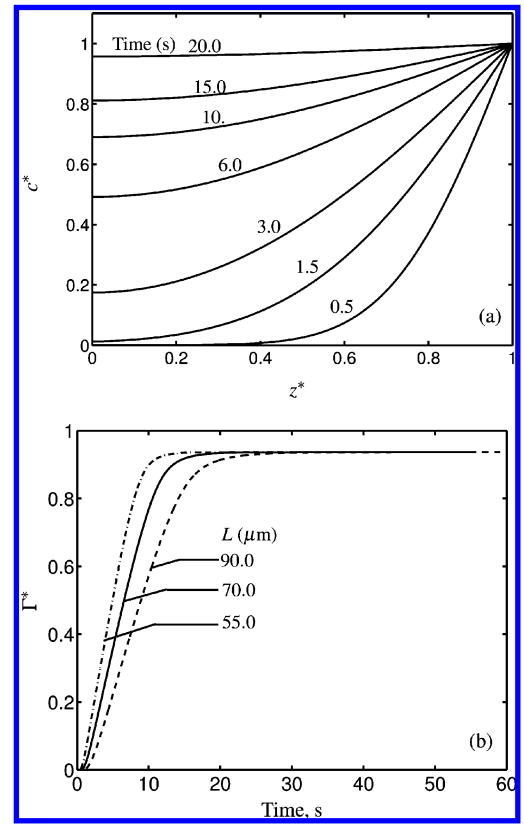

Figure 8. Solutions to the diffusion equation (eq 1) across a thin film of thickness L using the Langmuir isotherm. (a) Spatial and temporal variation of the concentration in the liquid film adjacent to the mica surface; $c^* = c/c_0$, where $c_0 = 15.0$ mol m^{-3}, $z^* = z/L$, where $L = 70.0 \times 10^{-6}$ m. (b) Amount adsorbed as a function of time for different values of L. In all cases, the diffusion coefficient is $D = 8.0 \times 10^{-10}$ m^2 s^{-1} and $c_{l1} = 1.0$ mol m^{-3}. At these conditions, a time lag of a few seconds is observed before film formation occurs.

Ward−Tordai equation, we observed that for values of D ranging from 5 to 8 $\times$ 10^{-10} m^2 s^{-1} and $c_{l1} = 1.0$ mol m^{-3}, 90% of saturation is established within 50−100 s. The influence of the diffusivity on $\Gamma^*(t)$ is illustrated in Figure 7b for $c_{l1} = 1.0$ mol m^{-3}. The analysis with the Ward−Tordai equation provides a suitable range for the parameters in the thin-film regime, and from the results shown in Figure 7, we observe that for $D = 8.0 \times 10^{-10}$ m^2 s^{-1} and $c_{l1} = 1.0$ mol m^{-3}, 90% of saturation is established within 60−100 s. Within the resolution of the film thickness measurements, we observe that the multilayer formation occurs beyond an immersion time of 60 s (Figure 3a). Solutions with the Ward−Tordai equation provide reasonable estimates of the parameters D and c_{l1} for film formation in the thin-film regime. On the basis of this, we use values of $D = 8.0 \times 10^{-10}$ m^2 s^{-1} and $c_{l1} = 1.0$ mol m^{-3} for prediction with the multilayer model. We note that the value of c_{l1} is important only in the thin-film regime which contributes only to the short time (stage I) evolution, and hence the multilayer model (discussed later) is relatively insensitive to changes in c_{l1}. The sensitivity of the model predictions to the values of c_{l1} and D are discussed later in the text.

Adsorption from a Thin Liquid Film. In order to estimate the liquid film thickness L, we solve the diffusion equation with the Langmuir isotherm in the thin-film regime. The variation of the amine concentration in the liquid film is shown in Figure 8a. Initially, the concentration near the surface is low, and the concentration builds up near the surface as the immersion time is increased. The concentration at the surface ($z = 0$) is used to calculate the amount adsorbed onto the mica surface through the isotherm (eq 7). Figure 8b shows the variation of Γ^* with immersion time for various values of L. Since molecules require a finite time to reach the mica surface, a small time lag in the system is observed before molecules begin to adsorb on the mica surface. Clearly, increasing L will increases this initial time lag. For the parameters $c_{l1} = 1.0$ mol m^{-3} and $D = 8.0 \times 10^{-10}$ m^2 s^{-1} (estimated from the Ward−Tordai solution), monolayer coverage is achieved between 10 and 30 s for L in the range of 55−90 μm. From the AFM experiments, we observe that the surface is covered with large sample spanning domains at 30 s. Using $L = 70$ μm and $D = 8.0 \times 10^{-10}$ m^2 s^{-1}, the diffusion time obtained is 2−3 s and indicates the time taken for the molecules to diffuse across the film of thickness L. Although we do not have experimental data at such short times, this estimate of the diffusion time is reasonable.

We next solve the diffusion equation with the two-site Langmuir model (eq 8) in order to predict the time evolution of the thin to thick film transition. Since we estimated the diffusivity D and c_{l1} from the Ward−Tordai solutions in the thin-film regime, the additional parameters for the multilayer adsorption model are c_{l2}, the concentration c_i in the two-site Langmuir model (eq 8), and the liquid film thickness L. From the experimental film thickness measurements, the ratio of the corresponding thick to thin film ratio is assumed to be equivalent to the ratio of Γ_{m2}/Γ_{m1}. From the experimental data, this ratio is estimated to be 25.0. Similar thin to thick film ratios have been observed in other systems such as adsorption of tetrethy-

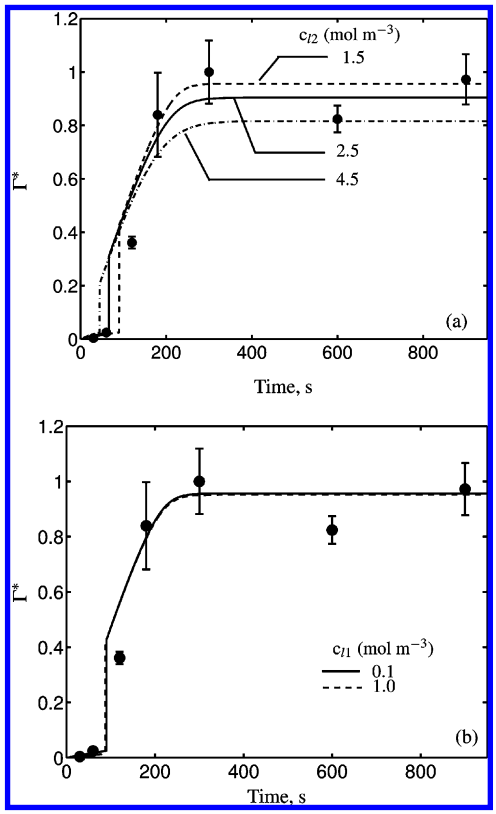

Figure 9. Solutions to the diffusion equation (eq 1) across a thin film of thickness L using the two-site Langmuir isotherm (eq 8), illustrating the time evolution of the amount adsorbed, $\Gamma^* = \Gamma/\Gamma_{m2}$. Variation of amount adsorbed for different values of the interaction parameter (a) c_{l2} and (b) c_{l1} in eq 8. Symbols refer to the film thickness data (scaled by the maximum height) obtained from AFM experiments. The model is able to capture the three stages of film growth observed in the experiments, and with the above parameters, the time taken for the thin to thick film transition is also captured. The time evolution of the adsorbed film is insensitive to the value of c_{l1}. Parameters used: (a)$c_{l1} = 1.0$ mol m^{-3}; (b) $c_{l2} = 1.5$ mol m^{-3}. In all cases, the diffusion coefficient is $D = 8.0 \times 10^{-10}$ m^2 s^{-1}, $L = 70.0 \times 10^{-6}$ m, and $c_i = 1.0$ mol m^{-3}.

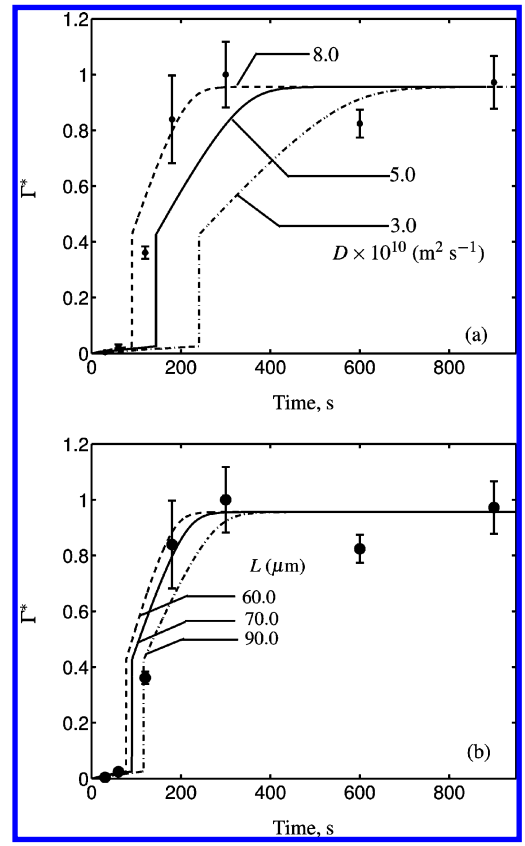

Figure 10. Solutions to the diffusion equation (eq 1) across a thin film of thickness L using the two-Γ-site Langmuir isotherm (eq 8), illustrating the amount adsorbed, $\Gamma^* = \Gamma/\Gamma_{m2}$. (a) Variation of the amount adsorbed for different values of the diffusion coefficient D in eq 8. (b) Variation of amount adsorbed for different values of the liquid film thickness L. Symbols refer to the film thickness data (scaled by the maximum height) obtained from AFM experiments. Parameters used: (a) $L = 70.0 \times 10^{-6}$ m; (b) $D = 8.0 \times 10^{-10}$ m^2 s^{-1}. In all cases, the interaction parameters are $c_{l1} = 1.0$ mol m^{-3}, $c_{l2} = 1.5$ mol m^{-3}, and $c_i = 1.0$ mol m^{-3}

lammonium perfluorooctylsulfonate (TEA-FOS) on hydroxylated germanium studied using total reflection FTIR spectroscopy.[46]

The concentration c_i is the bulk concentration at which the thin to thick film transition occurs in the adsorption isotherm. In order to determine this concentration, we carried out additional film thickness measurements by equilibrating the sample for sufficiently long (900 s) times to achieve equilibrium film formation for different bulk amine concentrations in the liquid. From these experiments, the thin to thick film transition was found to occur above $c_i = 1.0$ mol m^{-3}. We used this value of c_i for solutions of the diffusion equation. Defining $\Gamma^* = \Gamma/\Gamma_{m2}$, the solution for the diffusion equation as a function of c_{l2} for $L = 70.0$ μm and $c_i = 1.0$ mol m^{-3} is illustrated in Figure 9a. The first observation is that the model is able to capture the generic features observed in the thin to thick film transition as a function of the immersion time. In addition to increasing the equilibrium film thickness, decreasing c_{l2} was found to increase the time at which the thin to thick film transition was observed. Figure 9b shows that the time evolution of the adsorbed film is relatively insensitive to changes in the c_{l1} value which was determined from data in the monolayer or thin-film regime.

Figure 10 illustrates the manner in which the diffusion coefficient D and film thickness L influence the time evolution of the film thickness. The film thickness evolution is found to be quite sensitive to the value of D, and increasing the value of D at a fixed value of L shifts the thin to thick film transition toward the smaller immersion time, as shown in Figure 10a. Figure 10b illustrates the manner in which the film thickness L influences the time evolution of the film thickness. Increasing L at a fixed value of the diffusivity, D, only delays the time at which the thin to thick film transition is observed. Given the uncertainty associated in the data, particularly at short times, the modeling analysis in the section indicates that the two-site Langmuir model is able to capture the thin to thick film transition as well as the time at which this transition is observed. Although determining a unique set of parameters would require additional information on the adsorption isotherm as well as the diffusivity of the molecules in solution, our analysis suggests a suitable range of parameters which can be used to make quantitative predictions. For $L = 70$ μm, $D = 8 \times 10^{-10}$ m^2 s^{-1}, and $c_{l2} = 1.5$ mol m^{-3}, the model predictions are in excellent agreement with the observed experimental data, as illustrated in Figure 9.

We digress briefly at this point to discuss the relation between the solutions to the diffusion equation (eq 1) and the solutions to the Ward−Tordai equation (eq 6). The solutions to the diffusion equation (Figure 8) are obtained for an initial zero concentration of amine in the liquid film adjacent to the mica surface. Hence, the adsorbed film build up on the mica surface

is determined by the film thickness L, as illustrated in Figure 8. Alternately, one can assume that the initial amine concentration in the film corresponds to the bulk value (c_0). In this case, with a suitable choice of the initial concentration, the time evolution of Γ, obtained from solving the diffusion equation, is similar to that obtained using the Ward−Tordai solution as the situation is similar to the conditions under which the Ward−Tordai equation is solved. However, using the Ward−Tordai equation with the two-site Langmuir model or equivalent solutions of the diffusion equation with initial solute concentrations similar to those used while solving the Ward−Tordai equation did not yield the distinct transition from the thin to thick film as observed in the experiments. These solutions suggest that diffusion across a finite film of thickness L is the likely limiting step in the film evolution process.

Discussion

The film thickness measurements as a function of immersion time indicate the presence of three adsorption regimes. At short times $t < 60$ s, the film thickness is less than 1 nm, and this early stage of film formation is associated with large domain areas (Figure 4). In this regime, although the exact orientation of the molecules with the surface cannot be precisely determined, the domain height data suggest that the film is most likely to be present as a monolayer. We refer to this as the thin-film regime, where large sample spanning domains are observed. In the second stage (II), for immersion times above 60 s, there is a regime of rapid film growth, and the film thickness increases monotonically from 1 nm at 60 s to a maximum of 26 nm at 300 s. This thin to thick film transition occurs between 60 and 300 s. The AFM images illustrate this regime where a decrease in domain area is observed during the thin to thick film transition reaching a minimum area at 300 s when the film thickness evolution is seen to reach a maximum of 26 nm. Above 300 s, the film growth is complete, and the adsorbed amine molecules remain in the thick-film regime for longer immersion times, giving rise to stage III. The final stage of domain coarsening, which occurs above 300 s, is associated with an increasing domain area occurring on a thick film at the film−solution interface.

In stage I (Figure 3), associated with the thin-film regime, the precise morphology of the adsorbed film cannot be established. It is likely that in the initial stages where the adsorbed amount is low, the molecules adopt a surface-parallel configuration in order to maximize van der Waal interactions with the surface. As the coverage increases, the molecules would adopt a surface-perpendicular configuration with the amine group oriented toward the mica surface. This configuration would maximize interchain van der Waal interactions and is similar to the configuration observed during the chemisorption of thiol molecules on gold[52] and alkyltrichlorosilane molecules on silica.[38] In all cases, rinsing of the deposited film with the solvent (chloroform) resulted in a complete removal of the film, indicating that the bond between the deposited amine molecules and the mica surface is weak. Rinsing was carried out by immersing the amine-treated samples in pure chloroform for a few minutes. This and the fact that we were unable to detect any signature of a CH_2 stretch (post rinsing) in the FTIR spectra also suggest that the film is most probably a physiadsorbed film with a distribution of orientations relative to the mica surface.

Stage II is associated with a regime of rapid film growth, as illustrated in Figure 3, and the transition occurs from a thin to thick film with an increase in immersion time. At this point, we discuss film growth processes that occur in other systems such as vapor deposition as this will aid in interpreting the results observed in this study. During film growth, the morphology of the film is determined by two competing rate processes.[53,54] If the rate at which molecules impinge on the surface is faster than lateral surface diffusion, then the surface topology of the growing film is in the form of small islands. This regime is associated with rapid film growth giving rise to a rough surface topology. In our experiments, rapid film growth occurs during stage II, and the domain areas observed between 60 and 300 s reflect the surface topography captured during different stages of film growth. We note that the domain areas measured in stage II are during a transient regime of rapid film growth and would not, in general, be expected to depict a completely monotonic trend. Although some nonmonotonic variation is observed in the early times of stage II (Figure 5), for the small-area scans, a general decreasing trend in the domain area is observed during the latter part of this transient period of film growth. Furthermore, a minimum in the domain area is associated with the time at which the film attains the maximum observed thickness at 300 s. When the rate of incoming molecules is slow compared to surface diffusion, film growth is slowed or completed, and surface diffusion leads to growth of the domains observed in stage III. During this stage the smaller domains formed in stage II act as nucleation sites for lateral growth, coalescing to form larger domains, and a monotonic increase in domain area is observed, as illustrated in Figure 3. Above 300 s, corresponding to stage III, where the film growth is complete, coarsening occurs atop the adsorbed film.The AFM results indicate that film growth occurs by domain formation upon a growing bed. At all stages of the film growth, the heights of the domains were in the range of 1.5−2 nm, indicating that the domains are composed of monolayers consisting of molecules in a range of tilt angles. Pull-off forces on and between the domains did not reveal the presence of bare mica even during the early stages of immersion. The growth process that occurs by the formation of domains atop a preadsorbed multilayer film has the generic features of a Stranski−Krastanov growth process. Although the Stranski−Krastanov growth process is typically associated with the epitaxial growth of solid films, it has also been used to describe growth by island formation in films that do not grow epitaxially.[55]

Other system variables that can influence the adsorption at a fixed temperature are the concentration of the amine solution and the solution pH. In this study, experiments were carried out with the resultant pH of 9 obtained for a 15 mM octadecylamine solution with chloroform as the solvent. However, we carried out systematic experiments for a 900 s (long time) immersion with 1, 2, and 3 mM solutions. The corresponding film thickness were 0.7, 6, and 10 nm, respectively. In other surfactant adsorption studies, a nonmonotonic dependence of the surface excess (film thickness) was observed with increasing concentrations when the bulk concentration exceeded the critical micelle concentration (CMC).[46] In this study, the surface tension (28.2−28.6 N m^{-1}) was also found to be independent of concentration up to 20 mM, indicating that bulk micellization did not occur at the amine concentrations investigated in our study. The monotonic increase in the equilibrium film thickness as a function of bulk concentration is consistent with an adsorption process below the CMC. Hence, below the CMC, the ratio of the thick to thin film is expected to be directly proportional to the concentration of the amine solution as well as the interaction parameter c_{12} in the adsorption isotherm. This parameter, which is related to the strength of the interaction between amine molecules, is the leading factor for multilayer

film growth. A smaller value of c_{12} represents an increase in the interaction strength leading to thicker growth of the film (Figure 9a).

The temporal evolution of the distinct stages observed in the amine film growth is quantitatively captured using a diffusion-controlled model. In the absence of adsorption isotherm data, we used a two-site Langmuir isotherm model which assumes that the surface excess increases in two steps as the bulk concentration is increased.[56] The first step of the isotherm is associated with monolayer formation, and the second step is typically attributed to multilayers with a specific microstructure.[48] The parameters in the model are estimated based on the clear separations in the film thickness regimes, as observed in the experiments. The isotherm parameters corresponding to the monolayer regime as well as the transport parameters, which are the film thickness and diffusivity, are obtained from the time taken to form the monolayer. Using this procedure, the complete film thickness evolution is only dependent on a single additional parameter, c_{12}, in the two-site isotherm (eq 8). This route circumvents multiparameter fitting in order to compare model predictions with the experimental data. The model predicts the temporal evolution of the thin to thick film transition, in excellent agreement with the measured film thickness data, indicating that the process of film growth is limited by diffusion across a thin liquid film of thickness between 60 and 90 μm. The model captures the presence of two time constants, one associated with the time taken to form the thin film (<60 s) and the second, a longer time constant on the order of a few minutes, associated with multilayer growth.

Conclusion

The time evolution of the film growth and domain formation of octadecylamine films on a mica surface is studied using ex situ AFM, and a model based on the diffusion equation is used to predict the observed evolution of the adsorbed film. The film thickness for a given exposure time is measured by partially immersing the mica sample into the amine solution and measuring height changes across the mica−amine interface with large-area AFM scans. Film growth and domain evolution are found to occur in three distinct stages. In the first stage, which occurred for short exposure times (<60 s), the film thickness was less than 1 nm, and large sample spanning domains (~1 μm) were observed. The second stage (60−300 s) is associated with rapid film growth during which the adsorbed film reaches a maximum thickness of 26 nm. The domain morphology measured using the AFM reflects the topogographical changes that occur atop an adsorbed bed of amine molecules whose thickness is changing. Toward the latter part of this stage of rapid growth (200−300 s), a drop in the domain area is observed, reaching a minimum value at 300 s when the film growth is complete. Once the thick film regime is complete (>300 s), domain coarsening occurs, and the domain area increases monotonically from an initial area coverage of 38% at 300 s to over 75% at 900 s.

A diffusion-controlled model with a two-site Langmuir isotherm is able to capture the thin to thick film transition that is observed in the experiments. Using a suitable choice of parameters, good quantitative agreement is observed with the time evolution of the film thickness data obtained from AFM experiments. The model parameters are judiciously estimated using both the thin-film and thick-film adsorption data. Using the diffusion-limited model, we observe that the step in the time evolution of the film thickness is captured when a diffusion barrier is assumed to be present adjacent to the mica surface. The thickness of this diffusion barrier was found to lie in the range of 60−90 μm.

Lateral force and line profile AFM experiments only determine the domain heights and morphology associated with the surface of the adsorbed film. In combination with the novel film thickness determination method using partially immersed mica samples, we were able to determine the complete morphology of the adsorbed film and interpret the time evolution and domain growth in conjunction with the film thickness data in a consistent manner. The method provides a reliable method to track the evolution of the adsorbed films on mica surfaces and assumes special significance since other methods such as ellipsometry and FTIR are not easy to use with a mica surface. The method is generic and can be used ex situ for studying adsorption on solid surfaces, provided the substrate is sufficiently smooth to resolve the thickness of the deposited film.

Acknowledgment. One of us, K.G.P., thanks P. Savitha and H. S. Shamsundar for assisting with some of the AFM experiments. We thank N. Spencer, J. B. Pethica, O. P. Khatri, and R. R. Sahoo for several useful discussion during the progress of this work. We also acknowledge Indian Oil Corporation Limited for funding this work.

Supporting Information Available: AFM images of the amine−mica interface at lower immersion time. AFM images of domains with a large-area scan. Derivation of the Ward−Tordai equation and the method used to solve this equation. This material is available free of charge via the Internet at http://pubs.acs.org.

References and Notes

(1) Dantas Neto, A. A.; Castro Dantas, T. N.; Moura, M. C. P. A.; Barros Neto, E. L.; Duarte, L. J. N. *Ind. Eng. Chem. Res.* **2003**, *42*, 1994–1997.
(2) Pugh, R. J. *Miner. Eng.* **2001**, *14*, 1019–1031.
(3) Flater, E. E.; Ashurst, W. R.; Carpick, R. W. *Langmuir* **2007**, *23*, 9242–9252.
(4) Chandross, M.; Webb, E. B., I.; Stevens, M. J.; Grest, G. S.; Garofalini, S. H. *Phys. Rev. Lett.* **2004**, *93*, 166103.
(5) Ge, H.-H.; Zhou, G.-D.; Liao, Q.-Q.; Lee, Y. G.; Loo, B. H. *Appl. Surf. Sci.* **2000**, *156*, 39–46.
(6) Minami, I.; Kikuta, S.; Okabe, H. *Tribol. Int.* **1998**, *31*, 305–312.
(7) Ortiz, G.; Gonzalez, M.; Reviejo, A.; Pingarron, J. M. *Anal. Chem.* **1997**, *69*, 3521–3526.
(8) Waltermo, Å.; Sjöberg, M.; Anhede, B.; Claesson, P. M. *J. Colloid Interface Sci.* **1993**, *156*, 365–376.
(9) Rutland, M.; Waltermo, Å.; Claesson, P. *Langmuir* **1992**, *8*, 176–183.
(10) Pugh, R. J. *Adv. Colloid Interface Sci.* **1996**, *64*, 67–142.
(11) Tongcumpou, C.; Acosta, E. J.; Quencer, L. B.; Joseph, A. F.; Scamehorn, J. F.; Sabatini, D. A.; Yanumet, N.; Chavadej, S. *J. Surfactants Deterg.* **2005**, *8*, 147–156.
(12) Pandey, S.; Bagwe, R. P.; Shah, D. O. *J. Colloid Interface Sci.* **2003**, *267*, 160–166.
(13) Love, J. C.; Estroff, L. A.; Kriebel, J. K.; Nuzzo, R. G.; Whitesides, G. M. *Chem. Rev.* **2005**, *105*, 1103–1170.
(14) Ulman, A. *Chem. Rev.* **1996**, *96*, 1533–1554.
(15) Resch, R.; Grasserbauer, M.; Friedbacher, G.; Vallant, T.; Brunner, H.; Mayer, U.; Hoffmann, H. *Appl. Surf. Sci.* **1999**, *140*, 168–175.
(16) Richter, R. P.; Him, J. L. K.; Tessier, B.; Tessier, C.; Brisson, A. R. *Biophys. J.* **2005**, *89*, 3372–3385.
(17) Kurihara, K.; Mizukami, M.; Suzuki, K.; Oosawa, K. *Colloids Surf., A* **1996**, *109*, 375–384.
(18) Liu, Y. X.; Kang, E. T.; Neoh, K. G.; Tan, K. L.; Huang, C. C.; Liaw, D. J. *J. Appl. Polym. Sci.* **1999**, *74*, 816–824.
(19) Manne, S.; Gaub, H. E. *Science* **1995**, *270*, 1480–1482.
(20) Sharma, B. G.; Basu, S.; Sharma, M. M. *Langmuir* **1996**, *12*, 6506–6512.
(21) Ducker, W. A.; Wanless, E. J. *Langmuir* **1999**, *15*, 160–168.
(22) Sakai, H.; Nakamura, H.; Kozawa, K.; Abe, M. *Langmuir* **2001**, *17*, 1817–1820.
(23) Benítez, J. J.; Kopta, S.; Ogletree, D. F.; Salmeron, M. *Langmuir* **2002**, *18*, 6096–6100.

(24) Benítez, J. J.; Kopta, S.; Díez-Pérez, I.; Sanz, F.; Ogletree, D. F.; Salmeron, M. *Langmuir* **2003**, *19*, 762–765.
(25) Benítez, J. J.; Ogletree, D. F.; Salmeron, M. *Langmuir* **2003**, *19*, 3276–3281.
(26) Rozlosnik, N.; Gerstenberg, M. C.; Larsen, N. B. *Langmuir* **2003**, *19*, 1182–1188.
(27) Poptoshev, E.; Claesson, P. M. *Colloids Surf., A* **2006**, *291*, 45–50.
(28) Liu, J.; Messow, U. *Colloid Polym. Sci.* **2000**, *278*, 124–129.
(29) Lin, S.-Y.; McKeigue, K.; Maldarelli, C. *AIChE J.* **1990**, *36*, 1785–1795.
(30) Ward, A. F. H.; Tordai, L. *J. Chem. Phys.* **1946**, *14*, 453–461.
(31) Mysels, K. J. *J. Phys. Chem.* **1982**, *86*, 4648–4651.
(32) Yang, C.; Gu, Y. *Langmuir* **2004**, *20*, 2503–2511.
(33) Chang, C. H.; Wang, N.-H. L.; Franses, E. I. *Colloids Surf.* **1992**, *62*, 321–332.
(34) Horcas, I.; Fernandez, R.; Gomez-Rodriguez, J. M.; Colchero, J.; Gomez-Herrero, J.; Baro, A. M. *Rev. Sci. Instrum.* **2007**, *78*, 13705.
(35) Carson, G.; Granick, S. *J. Appl. Polym. Sci.* **1989**, *37*, 2767–2772.
(36) Bensebaa, F.; Ellis, T. H.; Badia, A.; Lennox, R. B. *J. Vac. Sci. Technol., A* **1995**, *13*, 1331–1336.
(37) Prathima, N.; Harini, M.; Rai, N.; Chandrashekara, R. H.; Ayappa, K. G.; Sampath, S.; Biswas, S. K. *Langmuir* **2005**, *21*, 2364–2374.
(38) Bierbaum, K.; Grunze, M.; Baski, A. A.; Chi, L. F.; Schrepp, W.; Fuchs, H. *Langmuir* **1995**, *11*, 2143–2150.
(39) Mellott, J. M.; Hayes, W. A.; Schwartz, D. K. *Langmuir* **2004**, *20*, 2341–2348.
(40) Bhushan, B.; Liu, H. *Phys. Rev. B* **2001**, *63*, 245412.
(41) Xiao, X.; Qian, L. *Langmuir* **2000**, *16*, 8153–8158.
(42) Asay, D. B.; Kim, S. H. *J. Chem. Phys.* **2006**, *124*, 174712.
(43) Farshchi-Tabrizi, M.; Kappl, M.; Cheng, Y.; Gutmann, J.; Butt, H.-J. *Langmuir* **2006**, *22*, 2171–2184.
(44) Ouyang, Q.; Ishida, K.; Okada, K. *Appl. Surf. Sci.* **2001**, *169–170*, 644–648.
(45) Morgenthaler, S.; Lee, S.; Zürcher, S.; Spencer, N. D. *Langmuir* **2003**, *19*, 10459–10462.
(46) Xing, R.; Rankin, S. E. *J. Phys. Chem. B* **2006**, *110*, 295–304.
(47) Reddy, J. N. *Introduction to the Finite Element Method*, 2nd ed.; McGraw-Hill: New York, 1998.
(48) Zhu, B.-Y.; Gu, T. *Adv. Colloid Interface Sci.* **1991**, *37*, 1–32.
(49) Bottani, E. J.; Bakaev, V. A. *Langmuir* **1994**, *10*, 1550–1555.
(50) Grey, T. J.; Nicholson, D.; Gale, J. D.; Peterson, B. K. *Appl. Surf. Sci.* **2002**, *196*, 105–114.
(51) Jung, L. S.; Campbell, C. T. *J. Phys. Chem. B* **2000**, *104*, 11168–11178.
(52) Xu, S.; Cruchon-Dupeyrat, S. J. N.; Garno, J. C.; Liu, G.-Y.; Kane Jennings, G.; Yong, T.-H.; Laibinis, P. E. *J. Chem. Phys.* **1998**, *108*, 5002–5012.
(53) Levine, S. W.; Engstrom, J. R.; Clancy, P. *Surf. Sci.* **1998**, *401*, 112–123.
(54) Doudevski, I.; Hayes, W. A.; Schwartz, D. K. *Phys. Rev. Lett.* **1998**, *81*, 4927–4930.
(55) Sandberg, H. G. O.; Frey, G. L.; Shkunov, M. N.; Sirringhaus, H.; Friend, R. H.; Nielsen, M. M.; Kumpf, C. *Langmuir* **2002**, *18*, 10176–10182.
(56) Mittal, K. L.; Shah, D. O. *Adsorption and aggregation of surfactants in solution*; Marcel Dekker, Inc.: New York, 2003.

JP9086255